INTERNATIONAL JOURNAL FOR NUMERICAL METHODS IN FLUIDS, VOL. 21, 129–139 (1995)

MATHEMATICAL MODELLING OF THE COUPLED REACTING BOUNDARY LAYER EQUATIONS

R. VILLASENOR

Sistemas de Combustión, Instituto de Investigaciones Electricas, Interior Internado Palmira, 62000 Cuernavaca, Morelos, Mexico

AND

J. Y. CHEN

Mechanical Engineering Department, University of California, Berkeley, CA 94720, U.S.A.

SUMMARY

A new numerical scheme for reacting axisymmetric jet flows formed between a fuel jet and co-flowing air has been developed. The model is mathematically described by a set of non-linear parabolic partial differential equations in two space dimensions, i.e. the boundary layer equations. The numerical scheme that the programme uses for solving the fully coupled conservation equations of mass, momentum, energy and species is a generalization of the discretization technique recently developed by Villasenor (*J. Math. Comput. Simul.*, **36**, 203–208 (1994)). Chemical production (and destruction) of the species is allowed to occur through N elementary reversible (or irreversible) reactions involving k species, although in the present model the reaction rates are evaluated with a simplified kinetic mechanism for a one-step global reaction. Thermal radiation is considered assuming an optically thin limit and adopting the grey medium approximation. Allowances are made for natural convection effects and variable thermodynamic and molecular transport properties. The performance of the model in solving the coupled aerodynamic and finite rate chemistry effects is tested by comparing model predictions with experimental data of Mitchell *et al.* (*Combust. Flame*, **37**, 227–244 (1980)) for a buoyant, laminar, diffusion axisymmetric methane–air flame.

KEY WORDS: numerical technique; boundary layer equations; reacting flow; full coupling; finite rate chemistry effects; thermal radiation effects

1. INTRODUCTION

In many axisymmetric jet combustion applications the axial molecular diffusion is practically negligible from moderate to high Reynolds numbers and the transversal pressure gradients are unimportant in the absence of swirl. A fairly good description of the flame structure and the aerodynamic characteristics of this kind of jet flow can be obtained with the boundary layer fluid flow equations. Depending on the degree of complexity of the transport and chemical reaction models, shear layer flows that couple the effects of fluid flow with detailed chemical reactions are computationally less expensive than two- or three-dimensional models. When the predominant gradients of the flow variables are perpendicular to the main direction of flow, it is not only inefficient but also unnecessary to consider multidimensional fluid dynamical effects, unless the difficulty of the transport and chemistry models is drastically reduced. Under the above circumstances the additional information a multidimensional model can offer may be comparable with a boundary layer flow simulation, as

CCC 0271–2091/95/020129–11

Received 20 June 1994
Revised 7 October 1994

Villasenor *et al.*[1] demonstrate for supersonic axisymmetric jet flames. In previous studies[1] a supersonic turbulent jet flow with non-premixed H_2–air combustion was modelled using a parabolic system of equations. Equilibrium and non-equilibrium chemistry models were used to simulate the chemical reactions. The turbulence was simulated with a modified κ–ε turbulence model to take into account the compressibility effects. The turbulence–chemistry interactions were quantified through a probability density function. The conditions in experiments reported for supersonic jet flames were used to evaluate the performance of the parabolic code in axisymmetric flows. The numerical results compared reasonably well with the measured data for velocity, major species and temperature. However, some discrepancies for major species were encountered between the predicted values and the experimental data in the fuel-lean side of the flame. Although the inconsistency was attributed mainly to the turbulent transport process, it was believed that by considering a different chemical reaction mechanism the numerical solution could be improved in that part of the flame. Also, to observe whether the scalar and velocity fields would have suffered possible changes by including the axial diffusion processes, the complete two-dimensional Navier–Stokes equations coupled with the species conservation equations were solved for the same non-premixed H_2–air flame.[2] Here the turbulence was simulated with an algebraic turbulence model and the turbulence–chemistry interactions were simplified through the assumption of weak turbulence. A mechanism with eight species and 18 steps was used to model the chemistry process. In general, both the boundary layer code and the two-dimensional model produced similar solutions for the scalar and velocity fields, except for the oxygen profiles and the relative levels of concentrations of minor species. The major difference between the boundary layer solution and the complete two-dimensional solution was that the latter could predict the penetration of O_2 into the fuel jet, with a substantial leakage at locations closer to the nozzle exit where the gas mixture temperatures are lower. On the other hand, the variations in the levels of minor species differed in their peak values and relative position in the flame. This peculiarity was due to small differences in the activation energies and in the number of steps of the chemical reaction mechanisms that each programme used. In view of that, in this work an axisymmetric reacting flow is modelled assuming that the boundary layer approximations are valid.

For the study of the mixing and chemical reactions of complex flow fields it is fundamental to predict the coupled effects of transport phenomena with chemical kinetics. A complete solution to the set of governing equations requires solving the terms for individual processes as well as accounting for the interaction among them. In recent years a number of efficient and stable numerical schemes[3–5] for the full two-dimensional conservation equations have appeared in the literature. However, very little work has been done on coupling the molecular diffusion processes with both chemical reaction and thermal radiation effects by using the boundary layer approximations. It is important to mention that the so-called 'look-up' table technique that has been widely used in the past[1,6–8] has made it possible to eliminate the stiffness problem that arises owing to the rates of reaction in the source terms of the species equations. The main reason for 'look-up' table implementation is that it facilitates the numerical integration of the discretized set of flow equations. The drawback here is that the velocity field has to be solved first so that the temperature and species concentrations can be determined afterwards. When a more complex kinetic reaction mechanism and flow fields are desired, this approach may yield inaccurate results owing to the uncoupling of the transport equations. It is therefore necessary, as has been recognized,[9] for a correct prediction of the mixing and chemical reaction of flow fields that the transport phenomena, chemical kinetics and thermal radiation effects be resolved simultaneously.

Recently Coltrin *et al.*[10] developed a FORTRAN programme called CRESLAF that predicts the velocity, temperature and species concentrations in two-dimensional channels. The programme accounts for finite rate chemical kinetics and molecular transport. The model employs the boundary layer approximations for the fluid flow equations. As a means to simplify the numerical procedure,

they recast the transport equations using a Von Mises transformation[11,12] in which the cross-stream co-ordinate is replaced by the streamfunction as an independent variable. It is important to point out that the streamfunction formulation has the inconvenience that the equations to be solved are integrodifferential equations. Hence the number of dependent variables increases with the presence of integral equations. However, more importantly, the structure of the Jacobian matrix is strongly affected. To circumvent this difficulty, a slightly different approach to the one followed by Coltrin *et al.*[10] is adopted here for the study of non-premixed laminar reacting flows.

In the new model the set of parabolic equations is first written in vector form and then discretized with a standard finite difference technique. This model is a generalization of the discretization technique recently developed by Villasenor.[13] As mentioned above, the significant advantage of the new model over the CRESLAF computer programme is the ability of the present method to eliminate problems associated with the structure of the Jacobian matrix. The integral equation arises because the recovery of the physical transverse co-ordinate is done through the definition of the streamfunction. The integral equation can be made to disappear if a further transformation is applied from the streamfunction co-ordinate domain to a non-dimensional streamfunction co-ordinate domain. The extra transformation has the great advantage that unconfined and confined jet flows can be indistinctly treated, whereas the CRESLAF code is unable to deal with unconfined jet flows. The mathematics software that CRESLAF uses is a modified version of DASSL. The computer package DASSL uses an implicit method that is most efficient for solving the stiff equations usually found in chemical kinetics problems. The newly developed model uses the original version of DASSL.[14]

Often the question arises as to whether a confined diffusion flame can be considered as an unconfined diffusion flame. Confined non-premixed flames often induce recirculation zones that tend to promote back mixing between the reactant and product. If such a recirculation zone exists, the boundary layer approximations may not be valid for describing the correct flame structure and the aerodynamic characteristics of the flow field. Instead, an elliptic equation solver is needed. The numerical techniques for solving a system of non-linear elliptic equations demand more elaborate methods of analysis than the one considered in this work. As a result, the computing time to simulate an elliptic flow is considerably greater than for a parabolic flow. None the less, the effect of the outer wall of a confined flame becomes negligible when the relation $\dot{m}_{air}/\dot{m}_{fuel} \gg (A/F)_{st}$ is met. Here $\dot{m}$ is defined as the mass flow rate and the right-hand side of the inequality stands for the stoichiometric air–fuel ratio. For the methane flame that will be studied here, $\dot{m}_{air}/\dot{m}_{fuel} = 60$ and its stoichiometric air–fuel ratio is 17. Thus the purpose of this work is also to verify that under the above condition a confined flame can be treated as an unconfined flame.

The rest of the paper is organized as follows. Section 2 first presents the model formulation and the discretized form of the non-linear partial differential equations, then introduces the chemical model for a simplified kinetics and finally describes and discusses thermal radiation effects. Section 3 is a presentation and discussion of the simulation of a confined, buoyant, laminar methane diffusion flame. Conclusions and suggestions are given in Section 4.

2. MODEL FORMULATION

2.1. Flame sheet model (FSM)

For practical non-premixed flames the flame thickness is small relative to the flame radius and a reasonable representation of the flame shape can be obtained by assuming that the reaction between fuel and air is infinitely fast.[15] In the limit of infinitely fast kinetics a thin exothermic reaction zone separates the fuel from the oxidizer. In the reaction zone the mixture is in stoichiometric proportions and the temperature and products of combustion are maximized. The infinitely fast chemistry

assumption implies that the instantaneous species concentrations are functions only of a conserved scalar,[16] the mixture fraction f. Assuming equal diffusivity for all species, the species conservation equations can be reduced to a single non-linear transport equation for mixture fraction with no source terms.[3,6,8]

The energy equation is expressed in terms of the total enthalpy h_T. The radiant energy flux and the energy flux due to thermal diffusion (Dufour effect) are not included in this model. The equal diffusivity assumption for all species implies that the Lewis number is unity. This means that the energy flux caused by interdiffusion (concentration gradients) is negligible. Furthermore, the viscous dissipation terms can be ignored for low-Mach-number flows. Then it follows that when there are two uniform reactant streams, a linear relationship among all conserved scalars exists. Hence the temperature can be recovered from the mixture fraction and the energy equation becomes redundant. However, to maintain generality in the FSM, the viscous dissipation and interdiffusion terms are included in the energy equation. The ideal gas equation of state serves to close the system of equations. The solution to the above set of non-linear, parabolic, partial differential equations leads to the determination of velocity, mixture fraction and total enthalpy. In vector representation the axisymmetric flow equations are given by

$$\mathbf{H}\frac{\partial \mathbf{U}}{\partial x} - \mathbf{G}\frac{\partial \mathbf{U}}{\partial \Psi} = \frac{\partial}{\partial \Psi}\left(\mathbf{Q}\frac{\partial \mathbf{U}}{\partial \Psi}\right) + \mathbf{F}, \tag{1}$$

where $\mathbf{U} = [u\ f\ h_T]^T$ is the vector of dependent variables and $\mathbf{F} = [-(\rho - \rho_\infty)g/\rho u\ \ 0\ \ 0]^T$ is the source vector. Here ρ is the gas mixture density, ρ_∞ is the outer flow density and u is the streamwise velocity. The configuration of the flame is such that x and Ψ are the axial and transversal co-ordinates respectively. The elements of the diffusion matrix $\mathbf{Q}$ in equation (1) are written as

$$\mathbf{Q} = \begin{bmatrix} \alpha\mu & 0 & 0 \\ 0 & \alpha\dfrac{\mu}{Pr} & 0 \\ \alpha\mu\left(1 - \dfrac{1}{Pr}\right)u & \alpha\displaystyle\sum_{k=1}^{K}\left(\rho D_k - \frac{\lambda}{C_p}\right)h_k\frac{\partial Y_k}{\partial f} & \alpha\dfrac{\lambda}{C_p} \end{bmatrix}. \tag{2}$$

Also in equation (1), $\mathbf{H}$ is the identity matrix and $\mathbf{G}$ is a diagonal matrix whose diagonal elements are all the same and equal to $\Lambda = -(a + b\Psi)$. The parameters a and b are related to the entrainment rates[11] at the inner (streamline ψ_i) and outer (streamline ψ_e) boundaries. The coefficient α in the diffusion matrix $\mathbf{Q}$ is defined as $\rho u r^2/(\psi_e - \psi_i)^2$.

For a CH_4–air laminar diffusion flame the recovery of the major species profiles follows from the conserved scalar f.[3,6,8] Of critical importance to this procedure is the location of the flame front f_{st}. For a CH_4–air diffusion flame, $f_{st} = 0{\cdot}055$. The location of the flame front is obtained from the conserved scalar at each axial location.

The finite difference representation of each term in equation (1) is obtained by considering an integration over a control area $\Delta A = \Delta x \cdot \Delta\Psi$. Between the grid points a linear interpolation formula is used when the integration is carried out in the transverse direction. An implicit method is used for all the dependent variables, with the elements in matrices $\mathbf{G}$, $\mathbf{Q}$ and $\mathbf{F}$ evaluated based on values at the upstream step. With the above finite difference procedure, equation (1) can be expressed in terms of algebraic equations at the ith nodal point as follows: $A_i^n U_{i-1}^{n+1} + B_i^n U_i^{n+1} + C_i^n U_{i+1}^{n+1} = D_i^n$. If we denote M as the number of finite difference equations (FDEs), then D_i^n is a $1 \times M$ source term matrix, A_i^n, B_i^n and C_i^n are $M \times M$ coefficient matrices and U_i^{n+1} is a $1 \times M$ dependent variable matrix. The coefficients A_i^n, B_i^n, etc. can be found in the literature[13] and will not be given again here.

2.2. *Differential/algebraic approach*

A first step to improve the FSM is to include finite rate chemistry effects. Chemical kinetics provides the coupling among the various chemical species concentrations and with the energy equations through the heat of reaction. In many combustion problems the kinetics terms dictate the characteristic space and the time space for which the numerical solution must be found. The widely differing scales of combustion processes lead to the well-known stiffness problem in solving the species concentration equations. When a finite rate chemistry model is needed for a better prediction of the combustion processes, an adequate numerical procedure must be implemented to eliminate numerical instabilities.

The numerical scheme for the FSM is incapable of handling stiff systems of equations. None the less, based on the same finite difference representation technique that was discussed in Section 2.1, it is possible to include finite rate chemistry effects by expressing the boundary layer equations as differential/algebraic equations (DAEs) in the context of numerically solving a system of ordinary differential equations. The solution procedure for DAEs was originally developed by Petzold[14] and was applied to the boundary layer equations for the first time by Coltrin *et al.*[17] through the method of lines.

The DAE approach can be used in conjunction with the finite volume formulation developed for the FSM. The main advantage of the present numerical method is that the Jacobian matrix retains its banded property and thus the problems related to computer storage are eliminated. Applying the discretization technique proposed by Villasenor,[13] equation (1) may be expressed at each grid node in the form

$$\begin{aligned}\mathbf{d}_i = &\left(\mathbf{H}\frac{\partial \mathbf{U}}{\partial x}\right)_i - \frac{1}{4\Delta\Psi_i}[(3G_i + G_{i+1})U_{i+1} + (G_{i-1} - G_{i+1})U_i - (3G_i + G_{i-1})U_{i-1}] \\ &- \frac{1}{\Delta\Psi_i}[q_{i+1/2}U_{i+1} - (q_{i+1/2} + q_{i-1/2})U_i + q_{i-1/2}U_{i-1}] \\ &- \frac{1}{4}\left(\frac{\Delta\Psi_{i+1/2}}{\Delta\Psi_i}F_{i+1} + 3F_i + \frac{\Delta\Psi_{i-1/2}}{\Delta\Psi_i}F_{i-1}\right) = \mathbf{0}. \end{aligned} \tag{3}$$

In equation (3), q_i is related[13] to Q_i and $\Delta\Psi_i$; the rest of the terms have already been defined in Section 2.1. In the DAE numerical scheme all the elements in matrices **Q** and **G** are zero except those of the main diagonal. For the former we have $Q_{jji} = \{\alpha u \ \dots \ \alpha\rho D_k \ \dots \ \alpha\lambda\}_i$, while for the latter $G_{jji} = \{\Lambda \ \dots \ \Lambda \ \dots \ C_p\Lambda\}_i$. The source terms of the momentum, species and energy equations are contained respectively in the source vector,

$$\begin{aligned}\mathbf{F} = \Bigg[&-\frac{(\rho - \rho_\infty)}{\rho u}g \ \cdots \ \frac{\dot{w}_k}{\rho u} \ \cdots \ -\frac{1}{\rho u}\sum_{k=1}^{K}\dot{w}_k W_k h_k \\ &+\frac{\rho u r^2}{(\psi_e - \psi_i)^2}\frac{\partial T}{\partial \Psi}\sum_{k=1}^{K}\rho D_k W_k C_{p_k}\frac{\partial \Gamma_k}{\partial \Psi} - \frac{1}{(\psi_e - \psi_i)}\frac{\partial (rQ_r)}{\partial \Psi}\Bigg]^{\mathrm{T}}. \end{aligned} \tag{4}$$

Here h_k and $\dot{w}_k$ represent the mixture enthalpy and reaction rate of species k respectively and the radiation heat flux is denoted by Q_r. With the momentum, species and energy equations a complete flame description is obtained having as the solution vector $\mathbf{U} = [u \ \cdots \Gamma_k \cdots \ T]^{\mathrm{T}}$. Notice that the energy equation has been expressed in terms of temperature T. As a result, the last term along the main diagonal of the matrix **H** is equal to the specific heat C_p instead of unity. The dependent variable in the species conservation equations ($\Gamma_k \equiv Y_k/W_k$) has been redefined in terms of the 'specific abundance' of species k, equal to its mass fraction divided by its molecular mass. The species k has a diffusivity D_k relative to the gas mixture.

The mathematics software that the model uses is called DASSL.[14] DASSL solves the equations in a marching fashion, starting from a given location $x_{\text{sheet}}^{\text{flame}}$ at which the initial profiles for the flow variables have been computed with the FSM and going towards the outer flow boundary. The code implements a variable-order, variable-step algorithm based on backward differentiation formula methods. The DASSL code chooses a sequence of time-like steps (x) such that the local truncation error in the marching direction is controlled to within a prespecified error tolerance. The general approach to using DASSL is to write a residual function $\mathbf{d}(x, \mathbf{U}, \partial\mathbf{U}/\partial x)$ as given by equation (3) at each mesh point, which is zero when the equations are satisfied. DASSL iterates on the solution at each time step until the approximate solutions $\mathbf{U}$ and $\partial\mathbf{U}/\partial x$ are sufficiently accurate and so $\mathbf{d}$ is zero.

2.3. The finite rate chemistry (FRCh) model

The major features inherent to laminar diffusion flame can often be predicted by using a simplified chemistry model. The simplified reaction mechanism must be capable of reproducing experimental flame properties over the range of operating conditions under consideration. Westbrook and Dryer[18] have reviewed some of the properties of simple reaction mechanisms and provide a list of single-step reaction rate parameters for a vast selection of hydrocarbons in premixed flames. The rate expression for a single reaction between methane and oxygen reported by Westbrook and Dryer[18] is used to compute the chemical source terms. For methane, $\dot{w}_{CH_4} = -1{\cdot}3 \times 10^8 \exp(-4{\cdot}84 \times 10^4/RT)(\rho Y_{CH_4}/W_{CH_4})^{-0{\cdot}3}(\rho Y_{O_2}/W_{O_2})^{1{\cdot}3}$. The units of the chemical source term are mol cm^{-3} s^{-1} and R is the universal gas constant (1·987 cal mol^{-1} K^{-1}). The reaction rate for methane is valid between the experimental flammability limits for equivalence ratio $0{\cdot}5 \leq \phi \leq 1{\cdot}6$. In the mixture fraction domain the flammability limits go from $f = 0{\cdot}0283$ (lean flame) to $f = 0{\cdot}085$ (fuel-rich). Outside this interval there is no production or destruction of species. The reaction rates of the other species are related through the stoichiometric coefficients by $\dot{w}_{O_2} = 2\dot{w}_{CH4}$, $\dot{w}_{H_2O} = -2\dot{w}_{CH_4}$ and $\dot{w}_{CO_2} = -\dot{w}_{CH_4}$. Nitrogen is the inert species in the flame and therefore $\dot{w}_{N_2} = 0$.

2.4. The thermal radiation model

Assuming the optically thin limit and adopting the grey medium approximation, the radiation heat flux appearing in the energy equation may be represented by

$$\frac{-1}{\psi_e - \psi_i}\frac{\partial(rQ_R)}{\partial\Psi} = 2k_p(2\sigma T^4 - B_w - B_\alpha). \tag{5}$$

In equation (5), k_p denotes the mean Planck absorption coefficient, σ is the Stefan–Boltzmann constant and B is given by $B = \varepsilon\sigma T^4$, where ε denotes the mean emissivity. At the boundary layer edge ε is that of the incoming air stream, while at the burner surface ε represents the joint emissivity of the burner surface and the gas mixture, herein numerical values of 0·2 and 0·1 have been used for ε_w and ε_α respectively.

The Planck mean absorption coefficient accounts for the absorption emission from the gaseous species CO_2 and H_2O and is expressed as

$$k_p = p[X_{H_2O}k_{p,H_2O}(T) + X_{CO_2}k_{p,CO_2}(T)]. \tag{6}$$

Here p (atm) is the pressure and $k_{p,k}$ (m^{-1} atm^{-1}) and X_k denote the mean absorption coefficient and mole fraction respectively of species k. In writing (6), the partial overlapping of the CO_2 and H_2O bands has been neglected as well as contribution to thermal radiation of CO. While it is generally recognized that the contribution to thermal radiation of CO is negligibly small in flames of hydrocarbon fuels, such contributions may be more important for flames of $CO/H_2/N_2$ fuels. A detailed discussion on this subject has been presented elsewhere.[19]

Table I. Polynomials coefficients for evaluation of k_{p,CO_2} and k_{p,H_2O}

$a_{k,n}$	CO_2	H_2O
a_0	$0{\cdot}22317 \times 10$	$0{\cdot}38041 \times 10$
a_1	$-0{\cdot}15829 \times 10$	$-0{\cdot}27808 \times 10$
a_2	$0{\cdot}13296 \times 10$	$0{\cdot}11672 \times 10$
a_3	$-0{\cdot}50707$	$-0{\cdot}28491$
a_4	$0{\cdot}93334 \times 10^{-1}$	$0{\cdot}38163 \times 10^{-1}$
a_5	$-0{\cdot}83108 \times 10^{-2}$	$-0{\cdot}26292 \times 10^{-2}$
a_6	$0{\cdot}28834 \times 10^{-3}$	$0{\cdot}37774 \times 10^{-4}$

The mean Planck absorption coefficients of CO_2 and H_2O required to evaluate the right-hand side of equation (6) are calculated with the formula

$$\log_{10}\left(\frac{k_{p,k}}{k_{p,k,ref}}\right) = \sum_{n=0}^{6} a_{k,n}\left(\frac{T}{300}\right)^n, \quad k = CO_2,\ H_2O. \tag{7}$$

In equation (7), T (K) is the temperature and $k_{p,k,ref}$ (m^{-1} atm^{-1}) is a reference value; the polynomial coefficients $a_{k,n}$ are given in Table I.

3. RESULTS

To demonstrate the importance of non-linear coupling among the PDEs for finite rate chemical kinetics and molecular transport, calculations of a laminar, axisymmetric, buoyancy flame for methane have been performed. The chemistry model consists of a simplified reaction mechanism for a one-step overall chemical reaction with variable transport properties. The thermodynamic and molecular diffusion coefficients are calculated with the CHEMKIN/TRANSPORT subroutines.[20] Measurements of a confined laminar diffusion flame[15] are used for comparison with the model predictions. In the experiment the fuel jet (pure methane) is supplied at a rate of 5·7 cm^3 s^{-1} and the outer flow (air) is maintained at 187·7 cm^3 s^{-1}. The experimental configuration is such that the radius of the inner jet is 0·635 cm, the radius of the outer oxidizer is 2·54 cm and the length of the tubular Pyrex shield is 30·0 cm.

The present work uses the numerical results[13] of the FSM for the same methane–air flame as that of Mitchell *et al.*[15] for comparison with the new model predictions. In the FSM a thin exothermic reaction zone separates the fuel from the oxidizer. The chemical reaction between fuel and oxygen is assumed to occur infinitely fast. Consequently, methane and oxygen cannot coexist. As a result, the FSM cannot predict the oxygen penetration into the central parts of the jet. Also, the radiation effects that are important in hydrocarbon flames are absent in the FSM computation.

In order to initialize the computation of the finite rate chemistry (FRCh) model, it is necessary to have a 'good' initial starting estimate. The initial starting profiles for temperature, velocity and chemical species are generated with the FSM. Assumed velocity and mixture fraction profiles are used to initialize the FSM. The FSM is run to some prescribed downstream axial location. In our case it is taken to be equal to 0·45 diameters downstream. Then the computation is switched to the FRCh calculation. Although the flammability limits for the simplified reaction mechanism are defined in the range $0{\cdot}028 \leq f \leq 0{\cdot}082$, the lower limit was taken to be 0·049, since the methane concentration decays abruptly to zero in the reaction zone and the reaction rates become undetermined. Eighty grid points across the jet are selected to completely solve this flow. The downstream integration is carried out up to 3·94 jet diameters downstream.

Figures 1 and 2 compare experimental and computational concentration profiles for both the FSM computation and the FRCh model of O_2 and CO_2 in the flame at heights of 1·2 and 5·0 cm respectively above the burner plate. Several features in Figures 1 and 2 are worth noting. The reaction zone clearly moves towards the centreline as the axial co-ordinate increases. In the two models the only region for fuel consumption of methane is at the fuel–oxygen interface where the highest levels of CO_2 are produced. The FSM oxygen concentration outside the flame region is near its inlet value and then drops to zero in the reaction zone. In contrast, the predicted oxygen distribution for the FRCh model diffuses all the way into the axis of the fuel injector to mix with unburned hydrocarbon and products of combustion. As shown in Figures 1 and 2, the radial mole fractions of oxygen predicted with the FRCh model are in better agreement with the measured data points than the numerical results computed with the FSM.

Figure 3 shows a comparison between the predicted temperature profiles calculated with the two models and the experimental values reported by Mitchell *et al.*[15] at locations $x/d = 0{\cdot}94$ and 3·94. Analysis of the temperature profiles in Figure 3 at the two selected axial stations shows that both models overpredict the temperature in the fuel-rich zone. However, the FSM overpredicts much higher temperatures. The overestimates of temperature inside the fuel-rich zone are caused mainly by the neglect of energy-absorbing pyrolysis reactions, as Keyes *et al.*[3] demonstrated by modelling a similar methane diffusion flame using a complex reaction mechanism. It is important to point out that the peak temperature of the FRCh results is lower than what the FSM predicts. Notice also the smooth spreading of the temperature distribution in the reaction zone. This behaviour is anticipated owing to the finite rates of reaction. Another interesting feature of the FRCh model is that by considering the radiation heat flux in the energy equation, a temperature drop of about 150 K is predicted relative to the adiabatic flame temperature predicted with the FSM.

Shown in Figure 4 are the computed velocity profiles for the two models and the velocity measurements of Mitchell *et al.*[15] at two different locations. The results predicted by the FSM differ

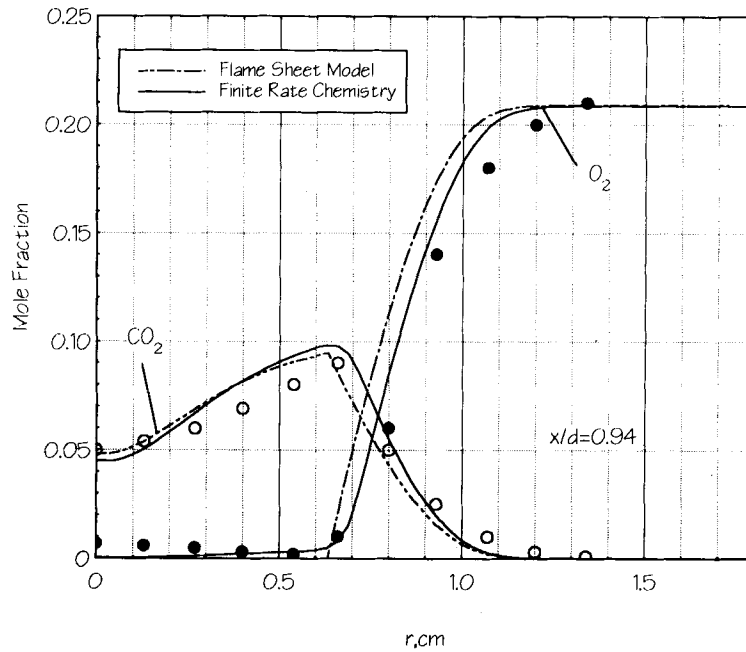

Figure 1. Radial concentration distributions of predicted and measured mole fractions of O_2 and CO_2 at axial location $x/d = 0{\cdot}94$

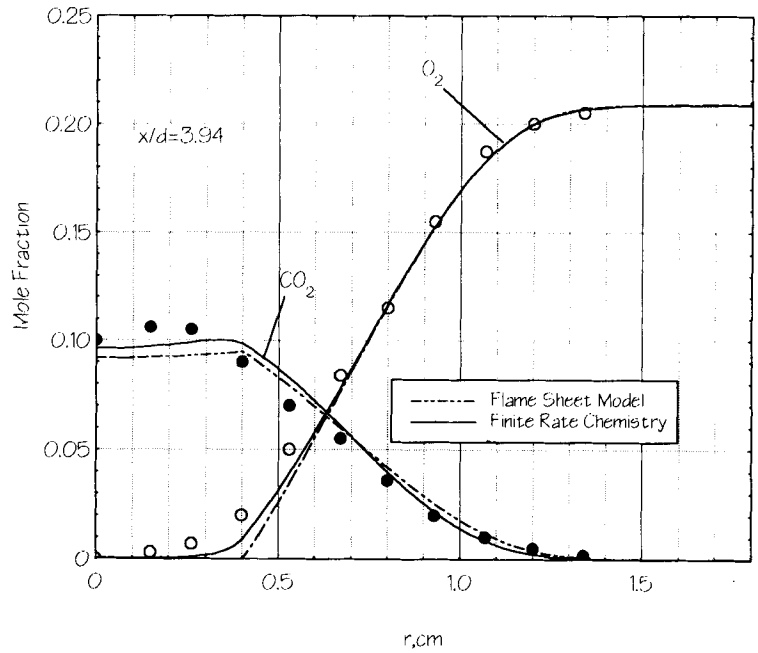

Figure 2. Radial concentration distributions of predicted and measured mole fractions of O_2 and CO_2 at axial location $x/d = 3{\cdot}94$

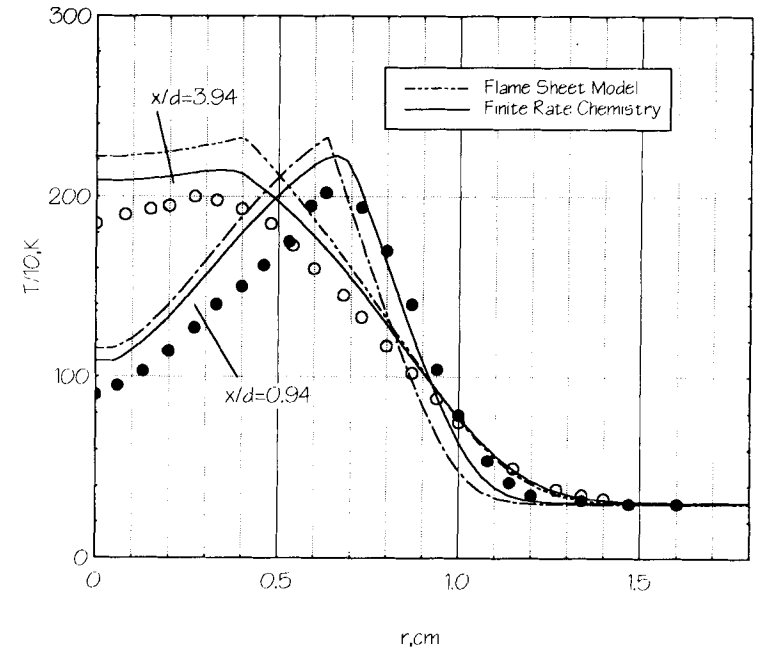

Figure 3. Comparison of predicted temperatures obtained with FSM and FRCh model and experimental temperature data at axial locations $x/d = 0{\cdot}94$ and $3{\cdot}94$

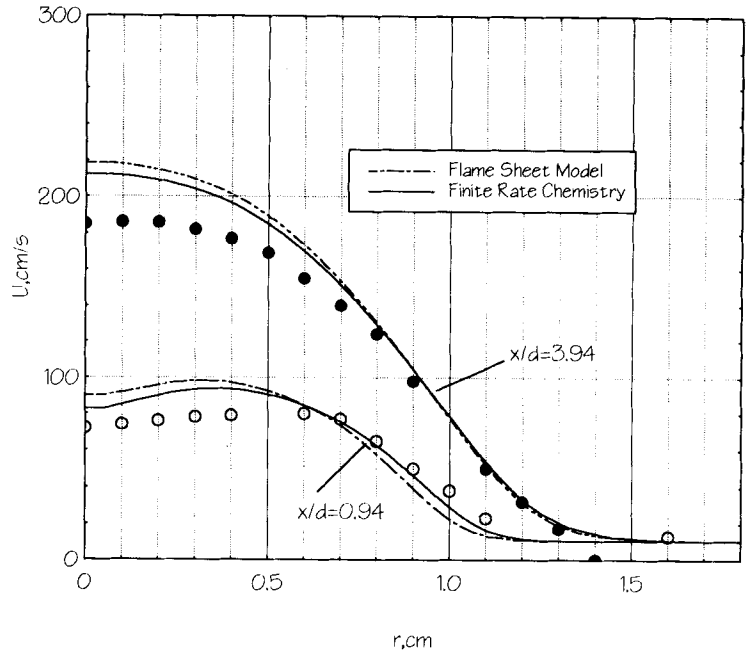

Figure 4. Comparison between numerical and experimental profiles of velocity at axial stations $x/d = 0{\cdot}94$ and $3{\cdot}94$

slightly from the solution obtained with the FRCh model in the fuel-lean and fuel-rich parts of the flame. The discrepancy is more evident on the fuel-rich side owing to a larger temperature increase with respect to the experimental values. It is observed that strong buoyancy effects are manifested by the substantial increase in the velocity of the gas mixture along the axis of symmetry. Notice also that in Figures 1–4 all the predicted profiles match perfectly the experimental data points in the outer parts of the flow field, indicating that the assumption of treating the confined flame as an unconfined one was correct.

4. CONCLUSIONS

A new numerical scheme, mathematically formulated for the boundary layer approximations, has been developed for solving the coupled momentum, energy and species conservation equations. The model predicts the velocity, temperature and concentration fields of any number of chemical species for a given kinetic mechanism. The thermal and aerodynamic fields established in a laminar methane–air flame, in which variable thermodynamic and molecular transport properties have been considered, are determined to test the performance of the model. Finite rate chemistry effects are included through a simplified reaction mechanism for the global reaction between CH_4 and air. Thermal radiation is considered assuming an optically thin limit and adopting the grey medium approximation.

The big advantage of the new model resides in the full coupling among the transport equations and the flexibility of this approach to include complex reaction mechanisms without altering significantly the structure of the code.

The results showed that a confined flame can be treated as an unconfined flame when the ratio of mass flow rate of oxidizer to mass flow rate of fuel exceeds the stoichiometric air–fuel ratio. Hence the problem can be stated in terms of parabolic equations instead of elliptic equations.

Finally, a note about the application of the developed code to industrial flames is in order. Most axisymmetric jets in combustion flows exist in a turbulent field and feature strong recirculation. This outstanding characteristic of industrial flames certainly poses some limitations on the usage of the present method for such flows.

REFERENCES

1. R. Villasenor, J. Y. Chen and R. W. Pitz, 'Modelling ideally expanded supersonic turbulent jet flows with non-premixed H_2–air combustion', *AIAA J.*, **30**, 395–402 (1992).
2. R. Villasenor, J. Y. Chen and R. W. Pitz, 'Interaction between chemical reaction and turbulence in supersonic non-premixed H_2–air combustion', *AIAA J.*, **30**, 2552–2254 (1992).
3. D. Keyes, D. Philbin and M. Smooke, 'Modification and improvement of software for modelling multidimensional reacting fuel flows', *Technical Report WRDC-TR-89-2056*, 1989, pp. 1–92.
4. J. L. Ellzey, K. J. Laskey and E. S. Oran, 'A study of confined diffusion flames', *Combust. Flame*, **84**, 249–264 (1991).
5. K. Prasad and E. W. Price, 'A numerical study of the leading edge of laminar diffusion flames', *Combust. Flame*, **90**, 155–173 (1992).
6. J. Janicka and W. Kollmann, 'The calculation of mean radical concentrations in turbulent diffusion flames', *Combust. Flame*, **44**, 319–336 (1982).
7. J. Y. Chen. 'Second-order conditional modeling of turbulent non- premixed flames with a composite PFE', *Combust. Flame*, **69**, 1–36 (1987).
8. J. Y. Chen and W. Kollmann, 'Segregation parameters and pair-exchange mixing models for turbulent non-premixed flames', *Proc. 23rd Int. Symp. on Combustion*, Orleans, 1990.
9. F. A. Williams, *Combustion Theory*, 2nd edn, Addison-Wesley, Redwood City, CA, 1985.
10. M. E. Coltrin, H. K. Moffatt, R. J. Kee and F. M. Rupley, 'CRESLAF: a Fortran program for modelling laminar, chemically reacting, boundary-layer flow in cylindrical or planar channels', *Sandia National Laboratories Report SAND93-0478*, 1993.
11. S. V. Patankar and D. B. Spalding, *Heat and Mass Transfer in Boundary Layers*, 2nd edn, Intertext Books, London, 1970.
12. J. Y. Chen, W. Kollmann and R. W. Dibble, 'Numerical computation of turbulent free-shear flows using a block-tridiagonal solver for a staggered grid system', *Proc. Eighteenth Ann. Pittsburgh Conf.*, Instrument Society of America, 1987.
13. R. Villasenor, 'A flame sheet calculation of a confined buoyancy laminar diffusion flame', *J. Math. Comput. Simul.*, **36**, 203–208 (1994).
14. L. R. Petzold, 'Differential/algebraic equations are not ODEs', *Sandia National Laboratories Report SAND81-8668*, 1981.
15. R. E. Mitchell, A. F. Sarofim and L. A. Clomburg, 'Experimental and numerical investigation of confined laminar diffusion flames', *Combust. Flame*, **37**, 227–224 (1980).
16. R. W. Bilger, 'Turbulent flows with non-premixed reactants', in P. A. Libby and F. A. Williams (eds), *Turbulent Reacting Flows*, Springer, New York, 1980, pp. 65–114.
17. M. E. Coltrin, R. J. Kee and J. A. Miller, 'A mathematical model of the coupled fluid mechanics and chemical kinetics in a chemical vapor deposition reactor', *J. Electrochem. Soc. Solid State Sci. Technol.*, 425–434 (1984).
18. C. K. Westbrook and F. L. Dryer, 'Simplified reaction mechanism for the oxidation of hydrocarbon fuels in flames', *Combust. Sci. Technol.*, **27**, 31–43 (1981).
19. J. Y. Chen, Y. Liu and B. Rogg, in N. Peters (ed.), *Reduced Kinetic Mechanisms for Applications in Combustion Systems*, Springer, New York, 1993, pp. 196–223.
20. R. J. Kee, J. A. Miller and T. H. Jefferson, 'CHEMKIN: a general-purpose problem-independent, Fortran chemical kinetics code package', *Sandia National Laboratories Report SAND80-8003*, 1980.